Reducing arsenic toxicity using the interfacial oxygen nanobubble technology in sediment remediation

Ying Tang[a,b], Meiyi Zhang[b], Jing Zhang[b], Tao Lyu[c], Mick Cooper[d], Gang Pan[b,d,*]

[a] *Chongqing Key Laboratory of Soil Multi-Scale Interfacial Process, Department of Soil Science, College of Resources and Environment, Southwest University, Chongqing 400715, P. R. China*

[b] *Research Center for Eco-Environmental Sciences, Chinese Academy of Sciences, Beijing 100085, P. R. China*

[c] *Cranfield Water Science Institute, Cranfield University, College Road, Cranfield, Bedfordshire, MK43 0AL, UK*

[d] *Integrated Water-Energy-Food Facility (iWEF), School of Animal, Rural, and Environmental Sciences, Nottingham Trent University, Nottinghamshire NG25 0QF, UK*

[*] *Corresponding authors: gang.pan@ntu.ac.uk (Gang Pan)*

Abstract

The worldwide arsenic (As)-bearing eutrophic waters may suffer from the dual conditions of harmful algal blooms and release of As, driven by algal-induced hypoxia/anoxia. Here, we investigate the use of interfacial oxygen (O_2) nanobubble technology to combat the hypoxia and control As exposure in simulated mesocosm experiments. It was observed that remediation of algal-induced hypoxia at the sediment-water interfaces (SWI) by application of O_2 nanobubbles reduced the level of dissolved As from 23.2 μg L^{-1} to <10 μg L^{-1} and stimulated the conversion of As(III) to the less toxic As(V) (65–75%) and methylated As (10–15%) species. More than half of the oxidation and all the methylation of As(III) resulted from the manipulation by O_2 nanobubbles of microbes responsible for As(III) oxidation and methylation. Hydroxyl radicals were generated during the oxidation of reductive substances at the SWI in darkness, and should be dominant contributors to As(III) abiotic oxidation. X-ray absorption near-edge structure (XANES) spectroscopic

analysis demonstrated that surface sediments changed from being sources to acting as sinks of As, due to the formation of Fe-(hydr)oxide. Overall, this study suggests that interfacial O_2 nanobubble technology could be a potential method for remediation of sediment As pollution through the manipulation of O_2-related microbial and geochemical reactions.

Keywords: Eutrophic waters; Arsenic oxidation; Nanobubble; Hypoxia remediation; Arsenic metabolism functional genes; Hydroxyl radicals

1. Introduction

Levels of Arsenic (As) are increasing in the environment and posing threats in surface water ecosystems (e.g. rivers and lakes) through both natural and anthropogenic activities (Weber et al., 2010; Zhang et al., 2018a). Drinking water directly derived from such contaminated sources poses a human health risk for more than 150 million people globally (Kay, 2011). Moreover, ~~As~~ bioaccumulation and magnification of As through aquatic foods web ~~magnification~~, and uptake it by crops through irrigation with As-contaminated water also significantly contribute to public health issues (Huang, 2016~~Zavala and Duxbury, 2008~~). ~~Thus, development of As mitigation strategies to achieve and maintain low As concentrations in surface waters is crucial towards environmental sustainability, food security and in safeguarding global human health.~~

In aquatic environments ~~surface waters~~ where the bottom water ~~benthic environment~~ is well-oxygenated, As is commonly bound with Fe, Mn, and organic carbon within the sediment (Couture et al., 2010). ~~However,~~ Harmful algal blooms (HABs) are

~~also~~ increasing in aquatic ecosystems globally, owing to increases in episodic eutrophication and as a consequence of global warming (Huisman et al., 2018; Pan et al., 2018). The subsequent oxygen (O_2) depletion by mineralization of senescent algal blooms induces hypoxia/anoxia at the sediment-water interfaces (SWI~~), potentially causing the mobilization of various nutrients and pollutants from sediment to water column~~ (Lei et al., 2019; Tang et al., 2019~~; Wang et al., 2018~~). Previous field investigations have demonstrated that eutrophication induced hypoxia/anoxia might favour the reductive dissolution of As(V)/As(III)-bearing iron oxides in the surface sediments, ~~biogeochemical cycling of As~~ and thus induce ~~its~~ endogenous release of As to the water column ~~from lake sediment~~(Hasegawa et al., 2009; Yan et al., 2016). ~~During algal induced periods of hypoxia/anoxia, As levels in eutrophic waters can exceed the drinking water limits (10 μg L^{-1}), set by the World Health Organization (WHO), by several orders of magnitude (Hartland et al., 2015; Martin and Pedersen, 2004).~~ Moreover, reduction of As(V) to As(III) (a more toxic As species) could be stimulated by the activity of indigenous As(V)-reducing~~tive~~ microbes under hypoxic/anoxic conditions (Tang et al., 2019). Therefore, combating the hypoxic/anoxic conditions at the SWI could be an efficient strategy by which to control As levels and toxicity in eutrophic surface waters.

Traditional oxygenation methods, such as deep water aeration and the artificial mixing of surface and bottom waters (Bierlein et al., 2017), have been reported to be effective to some extent. However, these approaches have been hindered when used in large and/or deep waters, due to their capital costs and energy consumption (Bormans et al., 2016; Funkey et al., 2014). The capital cost of installation of pumps in a deep water body is estimated to cost approximately €0.3 million/km^2 (Stigebrandt and Gustafsson,

2007; Zhang et al., 2021). Additional operational costs of nearly €0.2-0.25 million/km^2/year may be incurred, due to the continuous operation required during the summer season, or even the whole year, in order to maintain the O_2 supply and resultant nutrients/pollutants control at the SWI (Bormans et al., 2015; Johnston et al., 2011). Moreover, the induced massive hydraulic disturbance caused by traditional aeration methods through pumps may trigger the re-suspension of anoxic sediments. Such re-suspended sediments could release the long-term buried pollutants/nutrients back to the water column and increase the O_2 consumption (Bormans et al., 2015). Furthermore, the change of the status could affect the stable habitats for the benthic biota~~. even affect benthic biota and lead to increased O_2 consumption and secondary release of pollution/nutrients, resulting from the re-suspension of anoxic sediments~~ (Zhang et al., 2021).

In order to overcome these drawbacks, ~~an~~ the interfacial O_2 nanobubble technology has been developed and attempted to address this issue in a cost-effective and environmental-friendly way (Zhang et al., 2018b). ~~to~~ This approach utilises natural minerals loaded with O_2, which could deliver nanoscale O_2 bubbles (bubble size < 1 μm) after settling into the sediment surface by natural gravity~~, a cost-effective and environmental-friendly way (Zhang et al., 2018b)~~. The~~is~~ earlier study also demonstrated synergy between the diffusion of O_2 nanobubbles and retention of O_2 in the surficial sediment layer, which successfully reversed the hypoxic conditions and maintained high levels of dissolved O_2 (6 mg L^{-1}) at the SWI over a period of 4 months (Zhang et al., 2018b). The successful performance could be attributed mainly to the novel physical and chemical features of nanobubbles including long lifespan, high gas transfer efficiency,

and the capability to generate free radicals, as compared to larger bubbles (Atkinson et al., 2019; Lyu et al., 2019). ~~Following this concept, further studies have been conducted by different researchers, however, these have been mainly focused on the treatment of hypoxia/anoxia conditions (Yu et al., 2019), nutrient turnover control (including nitrogen and phosphorus) (Zhang et al., 2020; Zhang et al., 2021), and modulation of mineralization of organics (Shi et al., 2018).~~ However, ~~T~~the effects of interfacial nanobubble technology on the control, and biogeochemical cycling, of toxic metal pollutants, such as As, during sediment remediation have not, hitherto, been well understood.

Once the O_2 nanobubbles were delivered to the hypoxic/anoxic SWI through minerals acting as carriers, we expected that the resultant hypoxic/anoxic-oxic transition could trigger As(III) oxidation through both biotic and abiotic processes. On the one hand, the supply of substantially dissolved O_2 ~~supply~~ may have stimulated the growth of the indigenous As(III) oxidizing ~~ase~~ microbes and induced biotic oxidation of As(III) to less toxic As(V) (Maguffin et al., 2015), which is prone to be immobilized by iron oxides minerals (Luong et al., 2018). On the other hand, the abiotic process of As(III) oxidation may have been caused by the generated hydroxyl radicals (•OH), as a highly reactive and unselective oxidant, ~~generated~~ during the nanobubble treatment. Previous studies have proved that •OH could be generated along with the natural bursting of O_2 nanobubbles (Atkinson et al., 2019). Moreover, the oxygenation of anoxic sediment/water containing abundant ferrous minerals and reduced organic matter may also produce abundant •OH through Fenton or Fenton-like processes in darkness (Liao et al., 2019a; Liao et al., 2019b; Tong et al., 2016). ~~Compared to the biotic oxidation of As(III), the abiotic oxidation~~

process of As(III) is usually a rapid reaction that might occur within hours (Luong et al., 2018; Page et al., 2013; Tong et al., 2016). The accompanied variation in concentration and speciation of Fe and organic matter may influence their bioavailability to microbial activity (Tang et al., 2019; Zhu et al., 2017), and thereby indirectly affect the biotic oxidation of As(III). Thus far, the hypothesised biotic and abiotic mechanisms and their quantitative contributions on As speciation in eutrophic waters have not been investigated.

The goal of this study was to evaluate the effectiveness, and to reveal the mechanism for the mitigation of As pollution by interfacial O_2 nanobubble technology in a simulated eutrophic sediment-water system. The overlying water quality and As speciation were recorded in order to evaluate the performance of hypoxic/anoxic reversion and As immobilization at the SWI. As and Fe K-edge X-ray absorption near-edge structure (XANES) spectral analyses were used to investigate sequestration mechanisms of As in the sediment, and genes responsible for As metabolism (Tang et al., 2019) (i.e., As(III) oxidation (*aio*A), As(V) respiratory reduction (*arr*A), As(V) reduction (*ars*C), and As(III) methylation (*ars*M)) extracted from the SWI were quantified to aid in the understanding of the biotic processes of As transformation. Additionally, •OH generation and its effect on As oxidation were studied in order to evaluate abiotic effects on As speciation.

2. Materials and methods

2.1 Sample collection and construction of mesocosm columns

Lake water and sediments were collected from Lake Dianchi (Fig. S1), which is the sixth largest freshwater lake in China and, historically, has suffered from severe As

contamination and the annual occurrence of cyanobacterial blooms (Zhou et al. 2016). Concentrations of As in the sediment and water column have been recorded to reach 154 mg kg^{-1} and 7.23 μg L^{-1}, respectively (Tang et al., 2019). After transferring to the laboratory, the original lake water collected from Dianchi was filtrated through a 0.2 μm membrane (Sartorius AG, Germany), in order to minimize the background concentration of algal biomass prior to any treatment. Then the filtrated lake water (600 mL) and sediments (220 mL) were then placed in 24 plexiglass cylinders (∅64 mm, length 300 mm) in order to simulate water-sediment systems (Fig. S1). All of the mesocosm columns were stabilized under dark conditions for three weeks, then algal bloom scum (*Microcystis aeruginosa,* 250 mg dry weight L^{-1} water), collected from Lake Dianchi, was added to all columns and flocculated by starch-modified soil (Jin et al., 2019) and then allowed to settle under gravity to the sediment surface, in order to simulate algal-induced hypoxia/anoxia at the SWI.

2.2 Interfacial nanobubble materials preparation and operation

Both O_2 and N_2 nanobubble-modified zeolites were prepared by a previously-described method (Zhang et al., 2018b), the details of which are also included in the Supporting Information. After preparation of the algae biomass and of the zeolite materials, six groups of columns (four replicates of each) were prepared as (Table S1): i) the control group; ii) the pristine zeolite (Air-Ze) treatment group; iii) the N_2 nanobubble-modified zeolite (N_2-Ze) treatment group; iv) the O_2 nanobubble-modified zeolite (O_2-Ze) treatment group; v) the sterilized control (S-control) group; and vi) the sterilized O_2 nanobubble-modified zeolite (S-O_2-Ze) treatment group. Among these mesocosms, the

Air-Ze and N_2-Ze groups were designed to identify As transformations resulting solely from the physical capping treatment or from any synergistic effects accompanying nanobubble treatment, during the experimental period of 18 days at 25 °C under dark conditions. The S-control and S-O_2-Ze groups were sterilized prior to commencement of the experiment groups, to avoid any microbial contribution to the As transformation process to the greatest extent, as well as to aid in the identification of any abiotic effects. In these latter two groups, all materials, including sediments, water, zeolites and algae biomass were sterilized as described in our previous study (Tang et al., 2019). The experiment conditions for the different groups are summarized in Table S1 in the Supporting Information.

2.3 Sampling and measurement

In order to monitor water quality and As mobilization during the interfacial O_2 nanobubble treatment, DO (dissolved oxygen) and Eh (redox potential) at the SWI were measured at days 0, 2, 4, 7, 12 and 18. At the same time, the overlying water at 4 cm above the SWI was sampled from the columns in groups i-iv and filtered through a 0.45 μm membrane (Whatman, UK), to measure the total dissolved As and the As speciation, including As(III), As(V), and methylated As (i.e. monomethylarsonate (MMA(V)) and dimethylarsinate (DMA(V))). ~~Filtration by 0.45 μm membrane is a common method for the isolation of dissolved chemical species from overlying water and associated suspended solids (Johnston et al., 2011; Tang et al., 2019; Yan et al., 2016; Zhang et al., 2021).~~

Due to the clearly superior performance of O_2-Ze for As mitigation, the control (i)

and O_2-Ze (iv) groups were employed for further mechanistic investigations. Sediment porewater samples were collected by Rhizons MOM samplers (Rhizosphere Research Products B.V., Wageningen, The Netherlands) from 1 cm above the SWI to 4 cm below with 1-cm intervals, at days 0, 2, 4, 7, 12, and 18. As this lab-scale study was conducted in isolated, well-controlled columns, the effects of dissolved forms of Fe and organic matter as suspended particles and/or in the colloidal size range, during water sample analysis, can be neglected (Wu et al., 2001). Sediment porewater samples and the aforementioned overlying water samples were filtered through a 0.45 μm membrane prior to determination of dissolved organic carbon (DOC), dissolved Fe(II) and total dissolved Fe. At the conclusion of the experiment, the mixed sediments from depths of 0-2 cm (surface), 2-4 cm (middle) and below 4 cm (deep) were sampled in an anaerobic glove chamber. These sediment samples were used for determining total organic carbon (TOC), total Fe(II), total Fe (TFe), As(III) and total As (TAs) concentrations. From these data, the concentrations of Fe(III) and As(V) can be calculated by difference between total Fe(II) and TFe, and between As(III) and TAs, respectively. Additionally, surficial sediments from these two groups were analysed by Synchrotron Radiation microscopic X-ray Fluorescence (SR-μXRF) in order to obtain the distributions of As and Fe, and by XANES in order to quantify the major speciation of As and Fe bound in sediments under various redox conditions. The abundances of genes associated with As metabolism in the overlying water column, surficial and mid-depth sediments were also analysed for these two groups, in order to ascertain the biotic mechanisms of As speciation. Moreover, to further identify the different contributions of biotic and abiotic processes to As oxidation, overlying water and surface sediment samples from both sterilised groups (v and vi) were

also taken under the same aforementioned regime and measured for total As and As(V). These levels were then compared with those from the corresponding unsterilized groups. All details about methods of measurement may be found in the Supporting Information.

2.4 Hydroxyl radical determination

As support for the estimation of the effect of •OH on abiotic As oxidation, two batch experiments were further conducted in order to discriminate whether the •OH could be generated directly from bursting nanobubbles or by simple hypoxic sediment/water oxygenation. Because lake water usually contains other chemical species, such as reduced Fe and organic matter, which create the potential to generate •OH when exposed to O_2 (Liao et al., 2019a; Liao et al., 2019b; Tong et al., 2016), ultrapure water was used to identify the •OH forming capacity of bursting nanobubbles directly sourced from O_2-Ze materials. Specifically, samples of the prepared O_2-Ze materials (10 g) were placed into degassed ultrapure water (50 mL) in a sealed amber flask. A sample of the water was then immediately removed and again at 5 minutes (mins), 0.5 hour, 24 hours and 7 days, for measurement by electron spin resonance (ESR), of •OH production (Tong et al., 2016), details are shown in the Supporting Information. Moreover, given that O_2-Ze can support abundant dissolved O_2 for oxygenation at the SWI, oxygenation of sterilized sediment slurry was additionally conducted in order to qualitatively verify the production of •OH and its potential for As oxidation. The experimental setup was similar to that employed by Tong et al. (2016), with some modification. Briefly, sterilised sediment (30 g) and sterilised lake water (150 mL) were mixed and stored in an anaerobic chamber filled with nitrogen (99.999%), before stirring magnetically in an open amber flask for oxygenation

with dissolved O_2 from the air under dark conditions. Three treatment groups with three replicates for each were performed: (I) A blank group, carried out without oxygenation; (II) An O_2 group, conducted under continuous magnetic stirring of the slurry for oxygenation; (III) An O_2-ethanol group, to which was added ethanol (100 mmol L^{-1}) for •OH inhibition (Tong et al., 2016) accompanying the oxygenation. Slurry samples from groups I and II were taken at 5 mins and 30 mins and filtered through a 0.45 μm membrane prior to •OH determination by ESR (Tong et al., 2016), details are shown in the Supporting Information. In addition, at 0, 3, 7, 17, 24, and 48 hours after the oxygenation, slurry waters (filtered through a 0.45 μm membrane) from all groups were taken for the determination of As(V) and total As, as previously detailed.

2.5 Calculation

The total dissolved As concentrations during the 18-day experimental period were used to calculate total dissolved As fluxes across the SWI. The average flux of total dissolved As was evaluated according to the mass balance equation (Tang et al., 2019), and the accumulated total dissolved As flux over the 18-day experimental period was calculated using MATLAB 9.4 software (MathWorks, Inc, USA) by the trapezoidal method (Shi et al., 2018), based on the average flux data.

3. Results and discussion

3.1 Hypoxia and As mitigation

At the early stage, some labile, simple and low molecular weight carbon compounds, such as alcohols, ketones, sugars or amino acids, in the settled algal biomass and surface

sediments are easily been biodegraded (Catalán et al., 2017; Guillemette et al., 2013), leading to rapid O_2 consumption and a consequent swift decrease of the DO to 0.1 mg L^{-1} and Eh to -140 mV at day 2 (Fig. 1A and 1B). This hypoxic condition was maintained during the entire experimental period in the control system, which indicated the potential high risk to the aquatic ecosystem if this situation had occurred in natural waters (Pan et al., 2019). Sediment capping treatments, with pristine and modified zeolites, have previously been used for control of internal phosphorus loading through the blocking of buried anaerobic substances (e.g. reduced iron, sulfide and organic matter) (Li~~ao~~ et al., 2017). However, the physical barrier thus formed at the SWI exhibited limited effect on the remediation of hypoxia, which was indicated by the low levels of DO (<0.5 mg L^{-1}) and Eh (<-50 mV) observed in the Air-Ze and N_2-Ze groups throughout the duration of the experiment (Fig. 1). When O_2-Ze was applied and allowed to naturally settle to the sediment surface, it was observed to partly mix with the soft algal bloom scum and sediments at the SWI (O_2-Ze group). The effects of sediment capping and the sustainable O_2 nanobubble release from the O_2-Ze matrix gradually compensated for the O_2 consumption at the SWI, resulting in the increase of DO to 3.2 mg L^{-1} and Eh to 150 mV beginning from day 7. This clear reversal of hypoxia, consistent with the previous studies (Shi et al., 2018; Yu et al., 2019; Zhang et al., 2021), ~~could be~~ was directly visuali~~s~~zed by formation of a light brown-coloured oxic layer (~1 cm thickness) at the SWI after seven days (Fig. 1 and S2). The observation of such oxic layer was well aligned with the previous findings (Zhang et al., 2018b), up to 4-cm depth of sediments turned to light brown color after the treatment by O_2-Ze for 127 days. This oxic layer was formed by the downward penetration of O_2~~,~~ from O_2 nanobubbles~~,~~ into surficial sediments~~,~~. ~~which~~ It

could, furthermore, provide an element of physical isolation, preventing the upwards diffusion of reduced substances from the anoxic layer into the water column and subsequent consumption of O_2~~,~~. Therefore, the generated oxic layer was contributed ~~contributing~~ to an oxic condition persistent for weeks or even months (Zhang et al., 2018b).

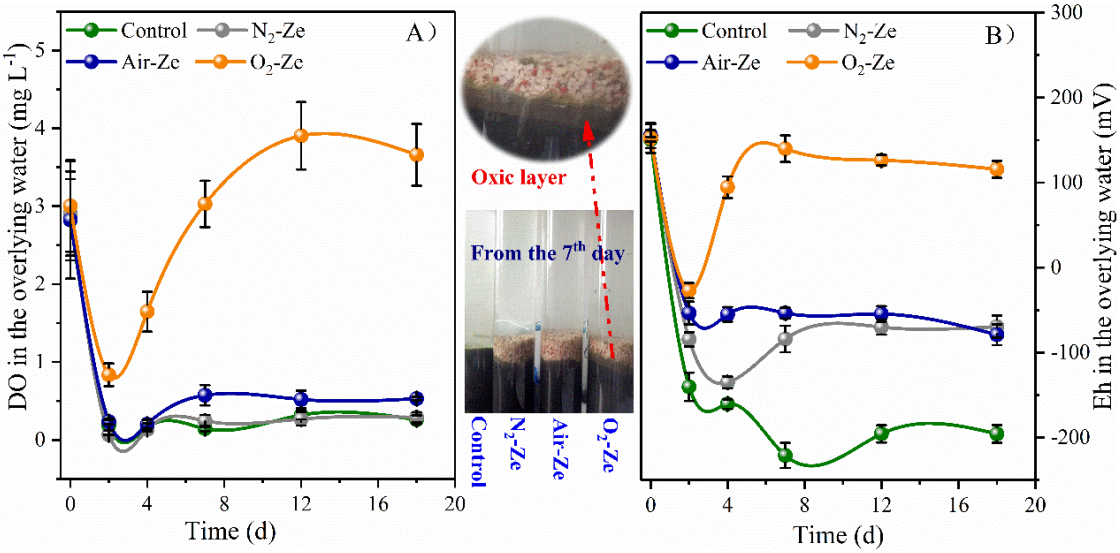

Fig. 1. Variation of DO (A) and Eh (B) in the overlying water during the experimental period

The simulated algal-induced hypoxia triggered an acute release of As from the sediment with total dissolved As levels reaching 23.2 μg L^{-1} in the overlying water by day 4 (Fig. 2A), ~~and~~ exceeding twice the WHO's recommended As safety limit (10 μg L^{-1}) (Yan et al., 2016). The total dissolved As levels in the overlying water from the Air-Ze and N_2-Ze groups were lower than those in the control group, but still remained higher than 10 μg L^{-1} during the experiment (Fig. 2A), indicating that the physical capping by zeolites alone was not enough to control the endogenous release of As. Accompanying the hypoxic-oxic transition in the O_2-Ze group, the total dissolved As in the overlying water remained at low levels, within the range of 6.97-9.72 μg L^{-1}. Moreover, the

289 cumulative total dissolved As fluxes from sediment to water switched from positive (net
290 As release) in the control (6.24 mg m^{-2}), N_2-Ze (2.88 mg m^{-2}) and Air-Ze (2.86 mg m^{-2})
291 groups to negative (net As retention) at -0.54 μg m^{-2} in the O_2-Ze group over the 18-day
292 incubation period (Fig. 2B), demonstrating the successful change of sediment from As
293 source to sink due to the synergistic effects of the formation of a physical barrier and the
294 effects of O_2 nanobubbles originating from O_2-Ze. It should be noted that the oxidizing
295 conditions at the SWI induced by O_2 nanobubbles also favoured As oxidation and
296 methylation. The predominant As species changed from the more toxic form of As(III) in
297 the control, N_2-Ze and Ze groups to lower toxicity forms of As(V) (65–75%) and
298 methylated As (MMA(V) and DMA(V)) (10–15%) in the O_2-Ze group (Fig. 2A) thus
299 further reducing the As exposure risk in the water column. Therefore, further investigation
300 into possible mechanisms was focused on the comparison between control and O_2-Ze
301 groups.

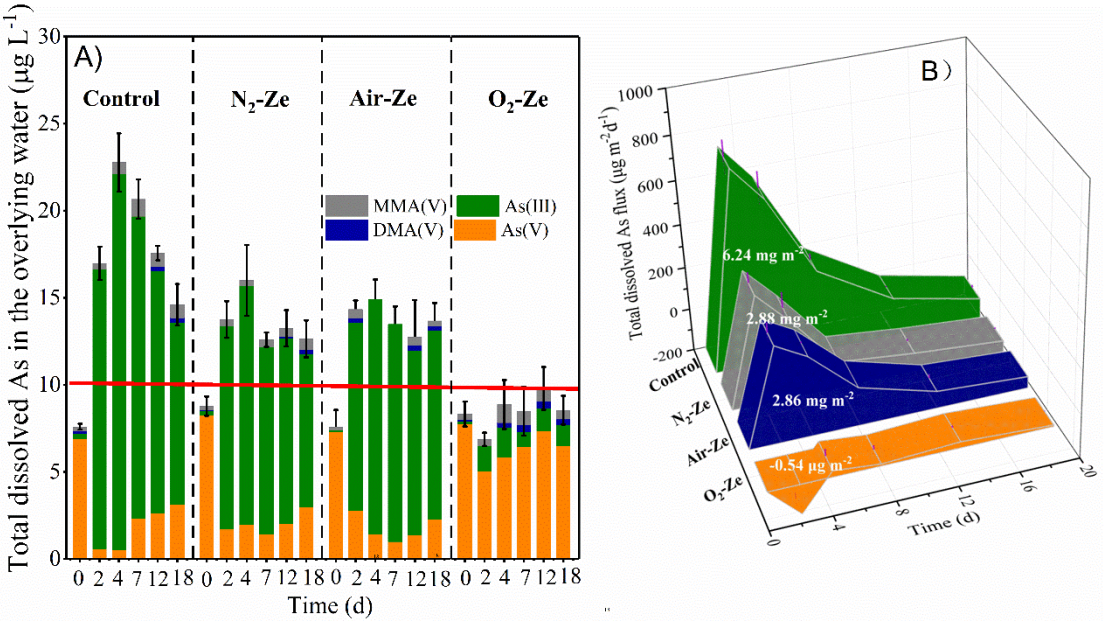

302

303 **Fig. 2.** As dynamics during the experimental period. (A) Total dissolved As in the overlying water.
304 The red line indicates the WHO's recommended As safety limits of 10 μg L^{-1} in drinking water.

(B) Total dissolved As flux across the sediment-water interface. The data appears in a white font in each bar, indicating the cumulative total dissolved As flux during the 18-day incubation period.

3.2 As mitigation controlled by geochemistry

It has long been recognised that the geochemical cycle of As is strongly linked to complex interactions, with co-mobilisation of some other elements, such as iron and carbon, also present in the sediment (Zhu et al., 2017). In the control group, accompanying the endogenous release of total dissolved As (mainly As(III)) (Fig. 2A), the algal-induced hypoxia also triggered the release of large amounts of DOC (Fig. 3A) and total dissolved Fe (mainly Fe(II)) (Fig. 3B) from sediments to the overlying water. The dynamics of DOC and total dissolved Fe in the overlying water (Fig. 3A and 3B) and sediment porewaters (Fig. ~~S2~~S3) followed the same trend and were ~~was~~ significantly correlated with concentration changes in total dissolved As in these waters ($P < 0.05$; Fig. 3C). This result indicated the occurrence of microbial reductive dissolution of As-bearing Fe oxides with subsequent As release (Zhou et al., 2016), as triggered by the intensified hypoxic conditions and the presence of an abundance of organic matter acting as an electron donor at the SWI (Postma et al., 2012; Tang et al., 2019). However, during treatment with O_2-Ze, a distinct decrease of DOC in the overlying water (Fig. 3A) ~~and organic carbon in surface sediments (Table S3)~~ was observed during the experimental period, when compared to the control. This may attribute to the oxidation reactions between DOC and dissolved O_2 or the possibly generated reactive oxidizing species (ROSs), such as •OH (Liao et al., 2019a; Page et al., 2013) at the SWI. The decrease of reactive organic carbon (e.g. glucose) at the SWI could further have inhibited the activity and growth of iron-reducing bacteria (Stuckey et al., 2016). Thus, oxidation of Fe(II)

occurred both in the overlying water (Fig. 3B) and in surficial sediments (Fig. S4B) compared to the control, and the regenerated Fe(III)-(hydr)oxides may have been responsible for As sequestration at the oxic SWI (Tong et al., 2016; Stuckey et al., 2016), leading to the combination of reduction in total dissolved As levels in overlying water and the inhibition of As release from surface sediments. This speculation was not only supported by the highly significant correlation between total dissolved Fe and As concentrations in water profiles (r = 0.631, P < 0.01; Fig. 3C), but also by a strong correlation between the spatial distribution of As and that of Fe in surface sediments in O_2-Ze group, observed through SR-μXRF analysis (Fig. 3D).

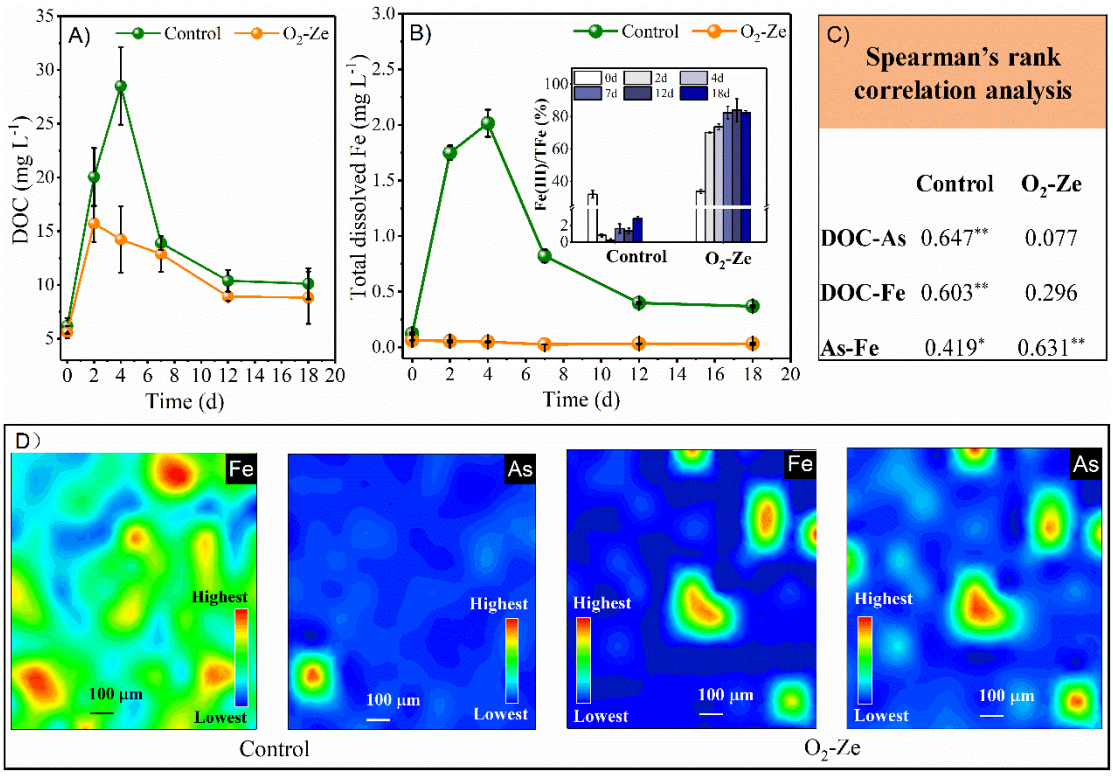

Fig. 3. Dynamic Geochemistry of As. (A) DOC (Dissolved Organic Carbon) in the overlying water; (B) Total dissolved Fe in the overlying water. The inset indicates the proportion of dissolved Fe (III) in the total dissolved Fe. (C) Spearman's rank correlation between total dissolved As, total dissolved Fe and DOC concentrations during the experimental period. Data for each correlation (n=24) consisted of concentrations taken from the overlying water and pore

water profiles. Values of $P < 0.05$ and < 0.01 indicate significant (*) and highly significant (**) correlations, respectively. (D) As and Fe distributions in surficial sediments, observed by SR-μXRF analysis.

In order to further quantify the variation of interaction between As and Fe in surficial sediments after O_2-Ze treatment, As and Fe K-edge XANES spectral analyses were conducted. Panels A and C of Fig.~~ure~~ 4 illustrate the linear combination fitting (LCF) of Fe and As K-edge XANES spectra of surface sediments sampled after completion of the simulation experiment, and Fig. 4B and 4D summarize the LCF results, respectively. The results indicated that the oxic layer, generated on the surficial~~e~~ sediments after O_2-Ze treatment, induced the rapid formation of ferrihydrite, the proportion of which increased from 6.9% to 38.1% (Fig. 4B). Ferrihydrite is one of the amorphous Fe(III)-oxyhydroxides that is ubiquitous in natural waters, especially at the redox boundaries of the SWI (Hoffmann et al., 2014). It is known to be an effective As absorbent, due to characteristics of nanometer-sized particles and high surface area (Tong et al., 2016; Stuckey et al., 2016). In this investigation, accompanied by the distinct oxidation of As(III) to As(V) in oxic surface sediments induced by O_2 nanobubbles (Fig. 4C and S~~34~~B), a significant increase (from 8.1% to 28.3%) in the generated As(V) adsorbed to ferrihydrite, compared with the control (Fig. 4D), was also observed. These results strongly confirmed that Fe-controlled sequestration was the primary inhibition mechanism of endogenous As release from As-bearing sediments under O_2-Ze treatment.

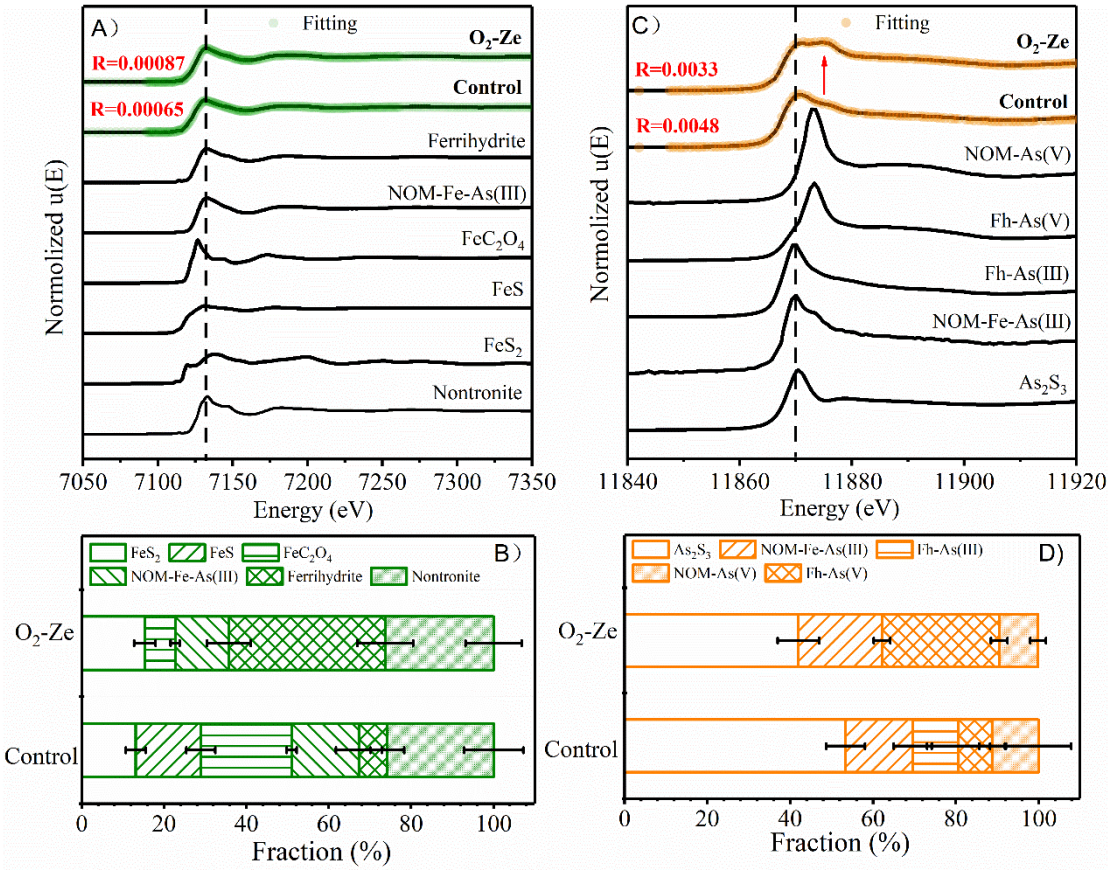

Fig. 4. As and Fe speciation in surface sediments. (A) and (C), Fe and As K-edge XANES spectra of the raw samples and reference compounds used for linear combination fitting (LCF) analyses, respectively. Experimental data are shown as solid black lines, and symbols represent LCF of the XANES spectra. R values show the mean square misfit between the data and the fit. (B) and (D), speciation of Fe and As in surface sediments, respectively. Speciation was obtained by LCF of K-edge XANES data and the component sums were normalized to 100%. Fh-As(III)/As(V) indicates ferrihydrite adsorbed As(III) or As(V).

3.3 Biotic- and abiotic-mediated As speciation

3.3.1 Biotic methylation of As

In unsterilized systems, the As methylation ratios along the whole experimental period achieved to 2.1-7.1% and 5.5%-14.7%~~A high methylation ratio of As~~ in the overlying water ~~in unsterilized systems was observed after~~ of control and O_2-Ze treatment ~~when compare to the control~~ group, respectively (Fig. 5A). However, similar As

methylation ratios (1.9-3.5%) were found in the overlying water in the two sterilized systems, i.e. S-O_2-Ze and S-control groups. In particular, the As methylation ratios were significantly higher in the unsterilized systems compare with the corresponding sterilized systems from day 7 ~~capping with O_2-Ze in the S-O_2-Ze group did not promote As methylation in the overlying water compared to the S-control group~~ (Fig. 5A). Th~~is~~ese results supported the premise that methylation of As(III) to MMA(V) and DMA(V) after capping with O_2-Ze was a microbially-mediated process (Maguffin et al., 2015). Known as an effective method of As detoxification, As methylation has been demonstrated to be catalysed by a family of As(III) S-adenosylmethionine methyltransferase enzymes encoded by the *ars*M gene (Zhu et al., 2017). There are more than 30,000 entries for *ars*M sequences in the NCBI database in members of all kingdoms, including both aerobic and anaerobic microbes (Zhang et al., 2013; Zhu et al., 2014). In our investigation, abundances of the *ars*M gene in the water column increased significantly from 4.51×10^6 to 5.46×10^6 copies L^{-1} after the O_2-Ze treatment (Fig. 5B)~~, demonstrating~~. It may attribute to the enhanced growth of As(III) methylated aerobic microbes~~,~~ under the oxic condition at SWI induced by capping with O_2-Ze. Those methylated microbes can further ~~which may have been~~ responsible for the methylation of As(III) to DMA(V) and MMA(V) in the overlying water (Fig. 2A) ~~(Zhu et al., 2014)~~.

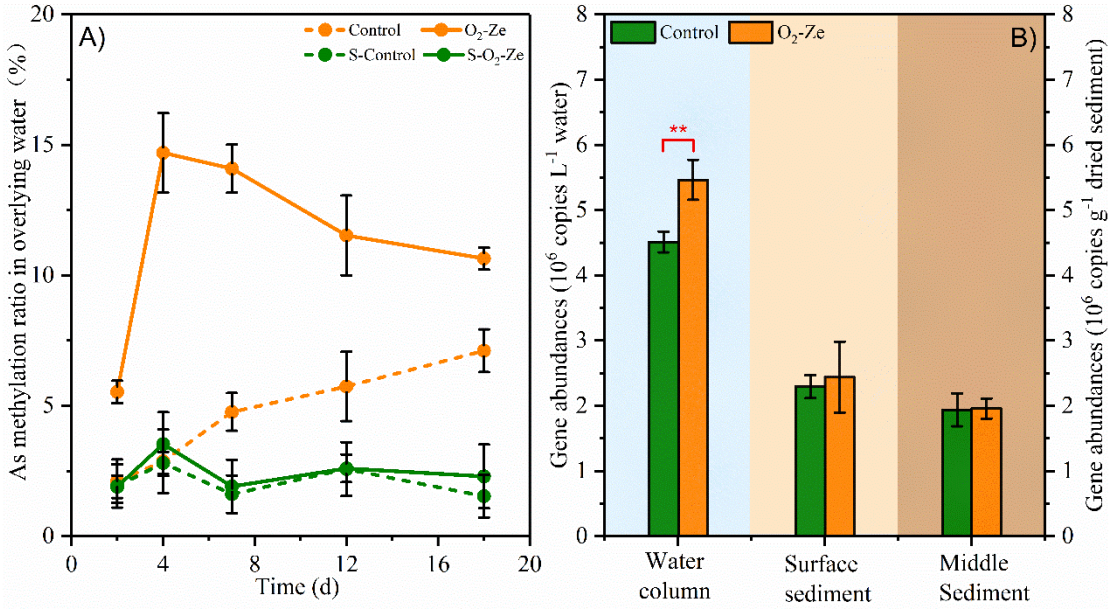

Fig. 5. Methylation of As at the SWI. (A) As methylation ratio in the overlying water in the sterilized and unsterilized systems. Methylation ratio of As was calculated by the concentration ratio of methylated As (i.e. DMA and MMA) and total dissolved As in the overlying water. (B) Gene abundances of *ars*M at the SWI. The symbol "**" represents $p < 0.01$ (independent t-test).

3.3.2 Biotic oxidation of As

Significantly higher As oxidation ratios in both overlying water and surface sediments were observed after hypoxia remediation by O_2 nanbubbles compared to the control in unsterilized systems (Fig. 6A and 6B). More importantly, the As oxidation ratio in the sterilised system under treatment by O_2-Ze also showed much higher levels, compared with the sterilised control group (Fig. 6A and 6B). These results supported the hypothesis that As oxidation induced by O_2 nanobubbles technology can be categorised as both a biotic process, mediated by functional microbial activity, as well as direct abiotic chemical oxidation at the oxic SWI. Generally, As oxidation in the sterilised systems can be considered an abiotic process, but one which accounted for 26.9-51.4% of the total As oxidation in the unsterilized system, based on the mass balance calculation (Fig. 6A and 6B). The remaining contribution of 52.5-73.1% could then be attributed to a biotic

processes. The biotic oxidation ~~through microbial metabolism~~ of As depends on the microbes capable of~~, involves~~ As(III) oxidation and As(V) reduction.~~, usually mediated by enzymes encoded by the *aio*A (oxidation), and the *arr*A and *ars*C (reduction) genes, respectively~~ As(III) oxidation is usually catalysed by As(III) oxidases encoded by *aio*A genes, and As(V) reduction involves respiratory pathway mediated by *arr*A genes and detoxification pathway mediated by *ars*C genes (Tang et al., 2019; Zhang et al., 2015). In comparison to the control groups, capping with O_2-Ze facilitated a highly significant increase in *aio*A gene abundances from 1.14×10^6 to 3.78×10^6 copies L^{-1} in the water column, and from 1.38×10^6 to 1.96×10^6 copies g^{-1} in surface sediments (Fig. 6C). This result indicated that the oxic SWI, induced by the introduction of O_2 nanobubbles, favoured the growth of indigenous As(III) oxidizing ~~ative~~ microbes, contributing to the biotic oxidation pathway of As from As(III) to As(V) (Fig. 6A and 6B) (Zhu et al., 2014). Simultaneously, the corresponding abundances of *arr*A and *ars*C genes at the SWI decreased significantly, implying that the oxic SWI also inhibited the microbial As(V) respiratory and detoxification reduction pathways (Zhang et al., 2015).

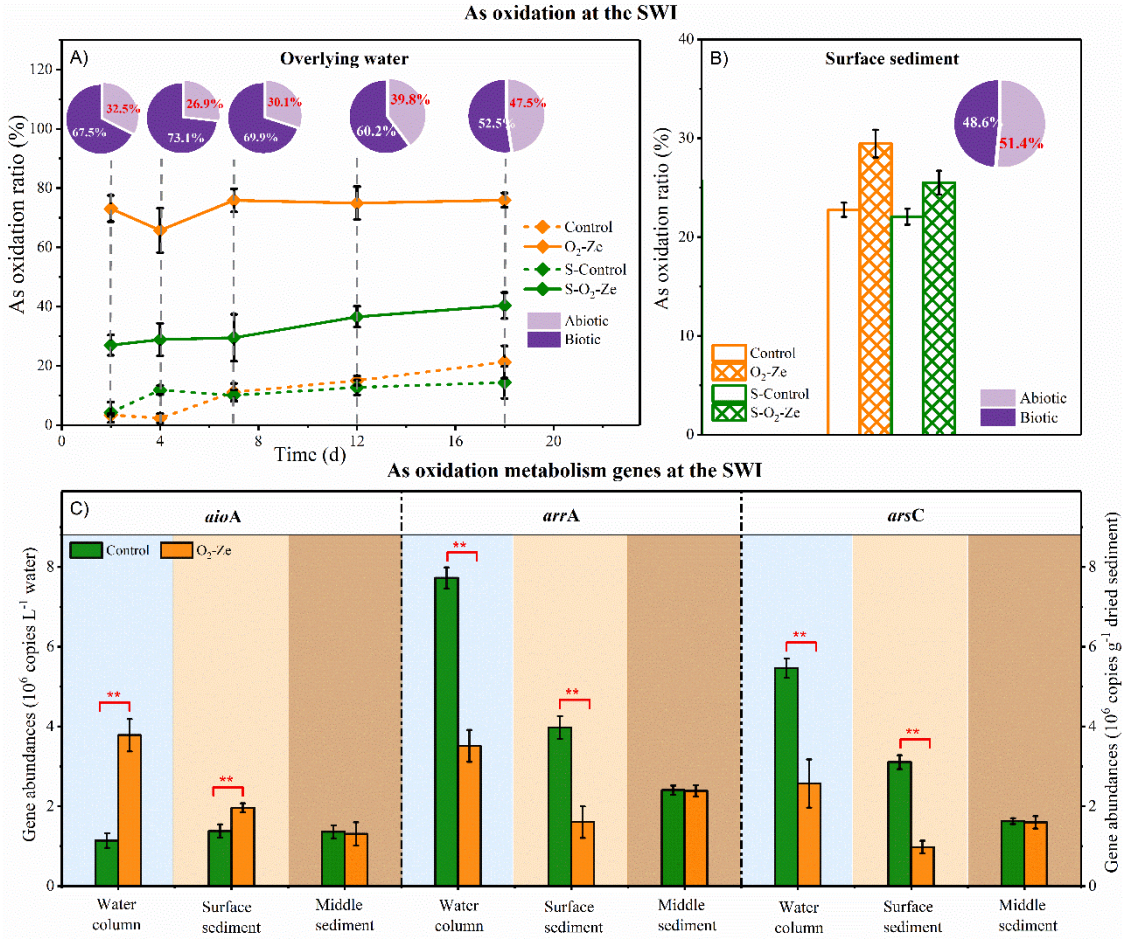

427

428 **Fig. 6.** Oxidation of As at the SWI. (A) As oxidation ratio in the overlying water for the sterilized
429 and unsterilized systems. It was calculated by the concentration ratio of dissolved As(V) and total
430 dissolved As in the overlying water. (B) As oxidation ratio in surface sediments for the sterilized
431 and unsterilized systems. It was calculated by the concentration ratio of As(V) and TAs in the
432 surface sediments. (C) Gene abundances of *aio*A, *arr*A and *ars*C at the SWI. The symbol"**"
433 represents $p < 0.01$ (independent t-test). The inset pie charts in (A) and (B) indicate the calculated
434 contributions of abiotic and biotic As oxidation.

435 ***3.3.3 Abiotic oxidation of As***

436 When O_2 nanobubbles were released from O_2-Ze at the hypoxic SWI, they may have
437 influenced the abiotic oxidation of As(III) by directly forming •OH during natural bubble
438 rupture (Atkinson et al., 2019), in addition to providing sufficient dissolved O_2 for
439 sediment/water oxygenation at the SWI (Fig. 1A). Therefore, we initially attempted to

measure the •OH forming capacity of pure water with O_2-Ze, but no distinct ESR •OH spectrum was detected (Figure S5). Given that the detection limit of ESR technique was usually 10^{-8} mol L^{-1} for paramagnetic species such as ROSs (Wang et al., 2011), this result indicated no, or extremely low, generation of •OH by natural bubble rupture from O_2-Ze, possibly due to the lack of •OH potentiating factors (e.g. UV irradiation or chemicals (such as H_2O_2)) in the waters (Liu et al., 2016). Therefore, it was considered that the dissolved O_2 supply was likely to be the dominant driver of abiotic oxidation of As(III) at the SWI.

Generally, abiotic oxidation of As(III) by dissolved O_2 is considered to be quite a slow reaction, with half-lives ranging from several months to a year (Smedley and Kinniburgh, 2002). However, this reaction can be catalysed in natural systems by the presence of redox-sensitive elements, such as Fe, Mn and C (Gorny et al., 2015). Recent studies have discovered the formation of •OH through Fenton or Fenton-like processes under dark conditions, once either Fe(II) or reduced organic matter in the anoxic water/sediments was exposed to, and oxidized by, dissolved O_2 (Tong et al., 2016). These reduced substances were abundant at the algal-induced hypoxic overlying water (Fig. 3A and 3B) and surficial sediments (Fig. S~~3~~4 and Table S3), but subsequently underwent rapid oxidation after encountering dissolved O_2 originating from O_2 nanobubbles in the O_2-Ze group, suggesting the possibility of generation of •OH at the SWI. To further verify production of •OH during the oxidation of hypoxic water/sediment at the SWI and to qualitatively clarify its potential for As abiotic oxidation, an oxygenation experiment was conducted using a sterilized sediment-water slurry. The results indicated that when the hypoxic slurry was exposed to dissolved O_2, an ESR spectrum, containing four peaks with

463 intensity ratios of 1:2:2:1, was observed, which could be compared to the ESR •OH
464 spectrum produced by the traditional Fenton process (Fig. 7A), implying the generation
465 of •OH.

466 Moreover, in ~~comparison with~~ the blank ~~control~~ group, the cumulative As oxidation
467 ratio was approximately 14% within 48 h (Fig. 7B). After exposure to dissolved O_2,
468 significantly higher ~~achieved~~ cumulative As oxidation ratio~~s~~ of nearly 44~~30~~% was
469 achieved in the water. However, the oxidation ~~corresponding~~ ratio~~s~~ sharply decreased to
470 24~~10~~% when ethanol, a •OH scavenger (Tong et al., 2016), was added during the
471 oxygenation process (Fig. 7B). These results confirmed that •OH, generated from the
472 oxidation of abundant reduced substances present in the sediment/water, rather than as a
473 direct result of nanobubble rupture, would be the predominant contributor to abiotic
474 oxidation of As in the O_2 nanobubble treatment. In addition to •OH, Fe(IV) may also play
475 a role in the residual abiotic oxidation of As(III). Several studies have reported that Fe(IV)
476 can be generated during interactions between Fe(II) and O_2 at neutral pH, leading to the
477 co-oxidation of As(III) in interfaces at natural redox environments (Ding et al., 2018; Hug
478 and Leupin, 2003). Thus, further research should focus on the in-site monitoring of •OH
479 and Fe(IV), in order to assessing their contributions to As speciation.

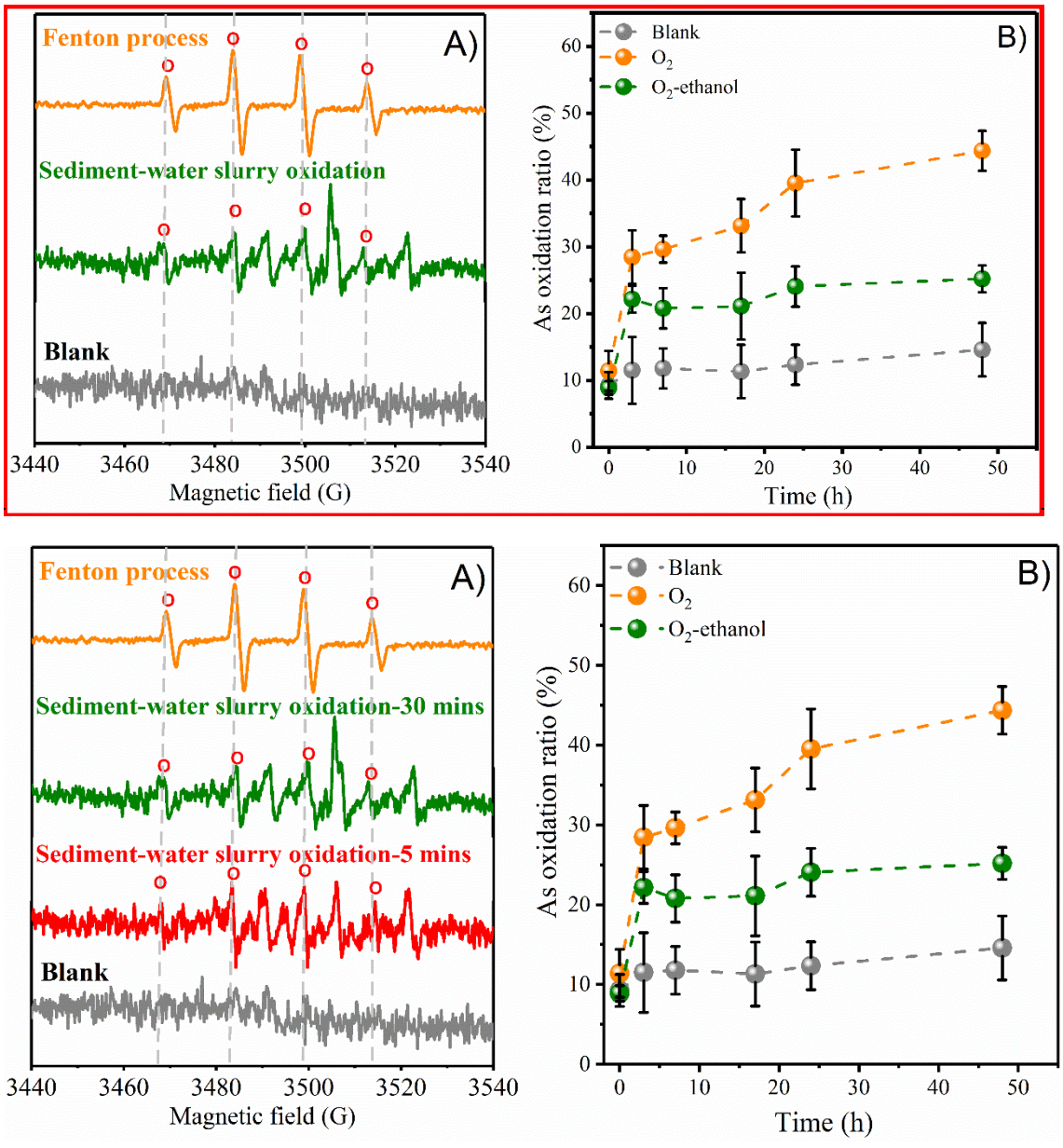

Fig. 7. Abiotic-mediated As speciation at the SWI. (A) ESR evidence of •OH production from oxygenation of sterilized sediment-water slurry. (B) As oxidation ratio in water during sterilized sediment-water slurry oxygenation (sediment/water=30 g/150 mL).

3.4 As fate under the treatment of O_2-Ze

In As-polluted eutrophic waters, where HABs problems are increasing (Hasegawa et al., 2009; Tang et al., 2019), anaerobic degradation of algae-induced organic matter at the SWI stimulates a contemporaneous release of As(III), Fe(II) and reduced organic matter into the water column (Fig. 2 and 3), leading to the risk of As pollution. Application

of O_2 -Ze at the hypoxic SWI can induce rapid remediation of hypoxia. The resultant oxidizing conditions favored the growth of indigenous As(III) methylated (carrying the *ars*M gene) and oxidative (through the *aio*A gene) microbes at the SWI. The former microbes catalyzed the biotransformation of As(III) to MMA(V) and DMA(V), and the latter catalyzed the biotic oxidation of As(III) to As(V). The As(III) oxidation process was also promoted by the reaction of As(III) with •OH, during which •OH can be produced by the oxidation of ferrous compounds and/or reduced organic matter in darkness. The resultant As(V), MMA(V) and DMA(V) have much lower toxicity than As(III) (Tang et al., 2019), which potentially reduce the risk of As exposure. Moreover, the rejuvenated ferrihydrite, at the oxidizing SWI, is highly efficient not only in stripping dissolved As(V) from the overlying water, but also in hampering the flux of As from sediments to the water column, thus further mitigating As pollution.

3.5 Environmental implications

Globally, HABs have been the cause of serious environmental disasters in hypereutrophic waters over recent years (Huisman et al., 2018). The resultant hypoxic/anoxic events have not only induced extensive mortality of benthos and fish, but have also caused elevated exposure of pollutants, including As (Tang et al., 2019). This study demonstrates that the proposed interfacial O_2 nanobubble technology has the capability to reverse the hypoxic conditions, by manipulating O_2-related microbial and geochemical processes to minimize the algal-induced As pollution risk in eutrophic waters. The hypoxia reversal effectiveness of this technology has proven to last for months in the earlier study (Zhang et al., 2018b), which may guarantee the long-term As

mitigation effect. Although a cost of €0.5-1.5 million per km^2 was roughly calculated by using the interfacial O_2 nanobubble technology for sediment remediation in a previous study (Zhang et al., 2021), this estimation was also based on a lab-scale experiment. Therefore, optimised methodology for the material preparation and longer-term experiments in large-scale systems should be further investigated, in order to move towards field application of the approach. This will enable a full cost-benefit analysis of the technology to be carried out. ~~However, in order to support the future real implementation, other potential factors, such as dosage of O_2-Ze and ecological impact of this technology, should be further in-situ studied.~~

Apart from the significant influence of O_2 nanobubbles on functional microbial activity of As, we also highlight the production of •OH in darkness, at the hypoxic SWI enriched with reductive substances and its dominant role in abiotic oxidation of As(III) during hypoxic-oxic transitions induced by dissolved O_2 from O_2 nanobubbles. This may provide insights for abiotic oxidative transformations of other redox-sensitive elements and chemical species (e.g. Hg, Cr, U, S , Fe, and antibiotics) in systems facing naturally- or artificially-hypoxic/anoxic-oxic transitions, for example, wetting and drying phenomena due to irrigation-evaporation cycles in wetlands (Gambrell, 1994) or tidal processes in estuaries and mudflats (Gonneea et al., 2014).

4. Conclusions

This study applied the use of interfacial O_2 nanobubble technology to combat the algal-induced hypoxia that achieves good performance for As mitigation in eutrophic waters. The hypoxic-oxic transition at SWI under O_2-Ze treatment manipulated microbes

responsible for As oxidation and methylation, leading to a conversion of As(III) to As(V) and methylated As species with less toxicity. It can also stimulate the dark formation of •OH, which further dominantly contributed to abiotic oxidation of As(III). The generated As(V) was sequestrated by Fe-(hydr)oxide under the oxic condition, making surface sediments changed from being sources to acting as sinks of As. Thus it suggested that the proposed technology could provide an eco-friendly and promising method for restoration of algal-induced As pollution in eutrophic waters.

Declaration of Competing Interest

The authors declare that they have no known competing financial interests or personal relationships that could have appeared to influence the work reported in this paper

Author contributions

G.P. and Y.T. conceived the experiments, which were carried out by Y.T., who also carried out data interpretation and drafted the manuscript. M.Y.Z. provided support for the synchrotron radiation measurements, genetic testing, and for manuscript preparation. T.L., J.Z. and M.C. contributed to the paper preparation, modification and language polishing.

Acknowledgements

This work was supported by the National Key R&D Program of China (2017YFA0207204, 2018YFD0800305), National Natural Science Foundation of China (42007339, 21377003), Fundamental Research Funds for the Central Universities (SWU119009), and Strategic Priority Research Program of the Chinese Academy of Sciences (XDA09030203). We thank Y. G. Zhu and G. X. Sun for help with

microbiological data analysis. We thank M. Tong for help with the design of the hydroxyl radical quenching experiments. We thank BSRF for providing the synchrotron beam time and L.R. Zheng and P.F. An for help in the collection of XANES data.

References

Atkinson, A.J., Apul, O.G., Schneider, O., Garcia-Segura, S., Westerhoff, P., 2019. Nanobubble technologies offer opportunities to improve water treatment. Accounts Chem. Res. 52(5), 1196-1205.

Bierlein, K.A., Rezvani, M., Socolofsky, S.A., Bryant, L.D., Wüest, A., Little, J.C., 2017. Increased sediment oxygen flux in lakes and reservoirs: The impact of hypolimnetic oxygenation. Water Resour. Res. 53(6), 4876-4890.

Bormans, M., Marsalek, B., Jancula, D., 2016. Controlling internal phosphorus loading in lakes by physical methods to reduce cyanobacterial blooms: a review. Aquatic Ecology 50(3), 407-422.

Bormans, M., Maršálek, B. and Jančula, D. (2015) Controlling internal phosphorus loading in lakes by physical methods to reduce cyanobacterial blooms: a review. Aquat. Ecol. 50(3), 407-422.

Catalán, N., Casas-Ruiz, J.P., von Schiller, D., Proia, L., Obrador, B., Zwirnmann, E., Marcé, R., 2017. Biodegradation kinetics of dissolved organic matter chromatographic fractions in an intermittent river. J. Geophys. Res-Biogeo. 122(1), 131-144.

Couture, R.M., Gobeil, C., Tessier, A., 2010. Arsenic, iron and sulfur co-diagenesis in lake sediments. Geochim. Cosmochim. Ac. 74(4), 1238-1255.

Ding, W., Xu, J., Chen, T., Liu, C., Li, J., Wu, F., 2018. Co-oxidation of As(III) and Fe(II) by oxygen through complexation between As(III) and Fe(II)/Fe(III) species. Water Res. 143, 599-607.

Funkey, C.P., Conley, D.J., Reuss, N.S., Humborg, C., Jilbert, T., Slomp, C.P., 2014. Hypoxia sustains cyanobacteria blooms in the Baltic Sea. Environ. Sci. Technol. 48(5), 2598-2602.

585 Gambrell, R.P., 1994. Trace and toxic metals in wetlands-a review. J. Environ. Qual. 23(5),
586 883-891.
587 Gonneea, M.E., Charette, M.A., Liu, Q., Herrera-Silveira, J.A., Morales-Ojeda, S.M.,
588 2014. Trace element geochemistry of groundwater in a karst subterranean estuary
589 (Yucatan Peninsula, Mexico). Geochim. Cosmochim. Ac. 132, 31-49.
590 Gorny, J., Billon, G., Lesven, L., Dumoulin, D., Made, B., Noiriel, C., 2015. Arsenic
591 behavior in river sediments under redox gradient: A review. Sci. Total Environ. 505,
592 423-434.
593 Guillemette, F., McCallister, S.L., del Giorgio, P.A., 2013. Differentiating the degradation
594 dynamics of algal and terrestrial carbon within complex natural dissolved organic
595 carbon in temperate lakes. J. Geophys. Res-Biogeo. 118(3), 963-973.
596 ~~Hartland, A., Andersen, M.S., Hamilton, D.P., 2015. Phosphorus and arsenic distributions~~
597 ~~in a seasonally stratified, iron- and manganese-rich lake: microbiological and~~
598 ~~geochemical controls. Environ. Chem. 12(6), 708-722.~~
599 Hasegawa, H., Rahman, M.A., Matsuda, T., Kitahara, T., Maki, T., Ueda, K., 2009. Effect
600 of eutrophication on the distribution of arsenic species in eutrophic and mesotrophic
601 lakes. Sci.Total Environ. 407(4), 1418-1425.
602 Hoffmann, M., Mikutta, C., Kretzschmar, R., 2014. Arsenite binding to sulfhydryl groups
603 in the absence and presence of ferrihydrite: a model study. Environ. Sci Technol.
604 48(7), 3822-3831.
605 Huang, J.H., 2016. Arsenic trophodynamics along the food chains/webs of different
606 ecosystems: a review. Chem. Ecol. 32(9), 803-828.
607 Hug, S.J., Leupin, O., 2003. Iron-catalyzed oxidation of arsenic(III) by oxygen and by
608 hydrogen peroxide: pH-dependent formation of oxidants in the Fenton reaction.
609 Environ. Sci. Technol. 37(12), 2734-2742.
610 Huisman, J., Codd, G.A., Paerl, H.W., Ibelings, B.W., Verspagen, J.M.H., Visser, P.M.,
611 2018. Cyanobacterial blooms. Nat. Rev. Microbiol. 16, 471-483.
612 Jin, X., Bi, L., Lyu, T., Chen, J., Zhang, H., Pan, G., 2019. Amphoteric starch-based
613 bicomponent modified soil for mitigation of harmful algal blooms (HABs) with
614 broad salinity tolerance: Flocculation, algal regrowth, and ecological safety. Water

Res. 165.

Johnston, S.G., Keene, A.F., Burton, E.D., Bush, R.T., Sullivan, L.A., 2011. Iron and arsenic cycling in intertidal surface sediments during wetland remediation. Environ. Sci. Technol. 45(6), 2179-2185.

Kay, P., 2011. Arsenic pollution: a global synthesis. Area 43(1), 118-119.

Lei, P.N., Luis M., Liu, Y.R., Zhong, H., Pan, K., 2019. Mechanisms of algal biomass input enhanced microbial Hg methylation in lake sediments. Environ. Int. 126, 279-288.

Li, Y.M., Fan, Y., Li, X.D., Wu, D.Y., 2017. Evaluation of zeolite/hydrous aluminum oxide as a sediment capping agent to reduce nutrients level in a pond. Ecol. Eng. 101, 170-178.

~~Liao, P., Li, W., Jiang, Y., Wu, J., Yuan, S., Fortner, J.D., Giammar, D.E., 2017. Formation, aggregation, and deposition dynamics of NOM-Iron colloids at anoxic-oxic interfaces. Environ. Sci. Technol. 51(21), 12235-12245.~~

Liao, P., Liang, Y., Shi, Z., 2019a. Impact of divalent cations on dark production of hydroxyl radicals from oxygenation of reduced humic acids at anoxic–oxic interfaces. ACS Earth Space Chem. 3(4), 484-494.

Liao, P., Yu, K., Lu, Y., Wang, P., Liang, Y, Shi, Z., 2019b. Extensive dark production of hydroxyl radicals from oxygenation of polluted river sediments. Chem. Eng. J. 368, 700-709.

Liu, S., Oshita, S., Kawabata, S., Makino, Y., Yoshimoto, T., 2016. Identification of ROS produced by nanobubbles and their positive and negative effects on vegetable seed germination. Langmuir 32(43), 11295-11302.

Luong, V.T., Canas Kurz, E.E., Hellriegel, U., Luu, T.L., Hoinkis, J., Bundschuh, J., 2018. Iron-based subsurface arsenic removal technologies by aeration: A review of the current state and future prospects. Water Res. 133, 110-122.

Lyu, T., Wu, S., Mortimer, R.J.G., Pan, G., 2019. Nanobubble technology in environmental engineering: revolutionization potential and challenges. Environ. Sci. Technol. 53(13), 7175-7176.

Maguffin, S.C., Kirk, M.F., Daigle, A.R., Hinkle, S.R., Jin, Q., 2015. Substantial contribution of biomethylation to aquifer arsenic cycling. Nat. Geosci. 8(4), 290-293.

~~Martin, A.J., Pedersen, T.F., 2004. Alteration to lake trophic status as a means to control arsenic mobility in a mine-impacted lake. Water Res. 38(20), 4415-4423.~~

Page, S.E., Kling, G.W., Sander, M., Harrold, K.H., Logan, J.R., McNeill, K., Cory, R.M., 2013. Dark formation of hydroxyl radical in arctic soil and surface waters. Environ. Sci. Technol. 47(22), 12860-12867.

Pan, G., Lyu, T., Mortimer, R., 2018. Comment: Closing phosphorus cycle from natural waters: re-capturing phosphorus through an integrated water-energy-food strategy. J. Environ. Sci. 65, 375-376.

Pan, G., Miao, X., Bi, L., Zhang, H., Wang, L., Wang, L., Wang, Z., Chen, J., Ali, J., Pan, M., Zhang, J., Yue, B., Lyu, T., 2019. Modified local soil (MLS) technology for harmful algal bloom control, sediment remediation, and ecological restoration. Water 11(6).

Postma, D., Larsen, F., Thai, N.T., Trang, P.T.K., Jakobsen, R., Nhan, P.Q., Long, T.V., Viet, P.H., Murray, A.S., 2012. Groundwater arsenic concentrations in Vietnam controlled by sediment age. Nat. Geosci. 5(9), 656-661.

Shi, W., Pan, G., Chen, Q., Song, L.-R., Zhu, L., Ji, X., 2018. Hypoxia remediation and methane emission manipulation using surface oxygen nanobubbles. Environ. Sci. Technol. 52(15), 8712-8717.

Smedley, P.L., Kinniburgh, D.G., 2002. A review of the source, behaviour and distribution of arsenic in natural waters. Appl. Geochem. 17(5), 517-568.

Stigebrandt, A., Gustafsson, B.G., 2007. Improvement of Baltic proper water quality using large-scale ecological engineering. AMBIO: A Journal of the Human Environment 36(2), 280-286.

Stuckey, J.W., Schaefer, M.V., Kocar, B.D., Benner, S.G., Fendorf, S., 2016. Arsenic release metabolically limited to permanently water-saturated soil in Mekong Delta. Nat. Geosci. 9(1), 70-76.

Tang, Y., Zhang, M., Sun, G., Pan, G., 2019. Impact of eutrophication on arsenic cycling in freshwaters. Water Res. 150, 191-199.

Tong, M., Yuan, S., Ma, S., Jin, M., Liu, D., Cheng, D., Liu, X., Gan, Y., Wang, Y., 2016. Production of abundant hydroxyl radicals from oxygenation of subsurface sediments.

676 Environ. Sci. Technol. 50(1), 214-221.
677 ~~Wang, L., Miao, X., Ali, J., Lyu, T., Pan, G., 2018. Quantification of oxygen nanobubbles~~
678 ~~in particulate matters and potential applications in remediation of anaerobic~~
679 ~~environment. ACS Omega 3(9), 10624-10630.~~
680 Wang, Z., Ma, W., Chen, C., Ji, H., Zhao, J., 2011. Probing paramagnetic species in
681 titania-based heterogeneous photocatalysis by electron spin resonance (ESR)
682 spectroscopy—A mini review. Chem. Eng. J. 170(2), 353-362.
683 Weber, F.A., Hofacker, A.F., Voegelin, A., Kretzschmar, R., 2010. Temperature
684 dependence and coupling of iron and arsenic reduction and release during flooding
685 of a contaminated soil. Environ. Sci. Technol. 44(1), 116-122.
686 Wu, J., Boyle, E., Sunda, W., Wen, L.S., 2001. Soluble and colloidal iron in the
687 oligotrophic north Atlantic and North Pacific. Science 293(5531), 847.
688 Yan, C., Che, F., Zeng, L., Wang, Z., Du, M., Wei, Q., Wang, Z., Wang, D., Zhen, Z., 2016.
689 Spatial and seasonal changes of arsenic species in Lake Taihu in relation to
690 eutrophication. Sci.Total Environ. 563–564, 496-505.
691 Yu, P., Wang, J., Chen, J., Guo, J., Yang, H., Chen, Q., 2019. Successful control of
692 phosphorus release from sediments using oxygen nano-bubble-modified minerals.
693 Sci.Total Environ. 663, 654-661.
694 ~~Zavala, Y.J., Duxbury, J.M., 2008. Arsenic in rice: I. Estimating normal levels of total~~
695 ~~arsenic in rice grain. Environ. Sci. Technol. 42(10), 3856-3860.~~
696 ~~Zhang, H., Chen, J., Han, M., An, W., Yu, J., 2020. Anoxia remediation and internal~~
697 ~~loading modulation in eutrophic lakes using geoengineering method based on~~
698 ~~oxygen nanobubbles. Sci. Total Environ. 714, 136766-136766.~~
699 Zhang, H., Huo, S., Yeager, K.M., Xi, B., Zhang, J., He, Z., Ma, C., Wu, F., 2018a.
700 Accumulation of arsenic, mercury and heavy metals in lacustrine sediment in
701 relation to eutrophication: Impacts of sources and climate change. Ecol. Indic. 93,
702 771-780.
703 Zhang, H., Lyu, T., Bi, L., Tempero, G., Hamilton, D.P., Pan, G., 2018b. Combating
704 hypoxia/anoxia at sediment-water interfaces: A preliminary study of oxygen
705 nanobubble modified clay materials. Sci. Total Environ. 637-638, 550-560.

706 Zhang, H., Lyu, T., Liu, L., Hu, Z., Chen, J., Su, B., Yu, J., Pan, G., 2021. Exploring a
707 multifunctional geoengineering material for eutrophication remediation:
708 Simultaneously control internal nutrient load and tackle hypoxia. Chem. Eng. J. 406,
709 127206.
710 Zhang, R,L., Sun, G.X., Zhu Y.G., 2013. Effects of microbial processes on the fate of
711 arsenic in paddy soil. Chinese Sci. Bull. 58(2), 186-193.
712 Zhang, S.Y., Zhao, F.J., Sun, G.X., Su, J.Q., Yang, X.R., Li, H., Zhu, Y.G., 2015. Diversity
713 and abundance of arsenic biotransformation genes in paddy soils from southern
714 China. Environ. Sci. Technol. 49(7), 4138-4146.
715 Zhou, Q., Zhang, Y., Lin, D., Shan, K., Luo, Y., Zhao, L., Tan, Z., Song, L., 2016. The
716 relationships of meteorological factors and nutrient levels with phytoplankton
717 biomass in a shallow eutrophic lake dominated by cyanobacteria, Lake Dianchi from
718 1991 to 2013. Environ. Sci. Pollut. Res. 23(15), 15616-15626.
719 Zhu, Y.G., Xue, X.M., Kappler, A., Rosen, B. P., Meharg, A. A., 2017. Linking genes to
720 microbial biogeochemical cycling: lessons from arsenic. Environ. Sci. Technol.
721 51(13), 7326-7339.
722 Zhu, Y.G., Yoshinga, M., Zhao, F.J., Rosen, B.P., 2014. Earth abides arsenic
723 biotransformations. Annu. Rev. Earth Pl. Sci. 42(1), 443-467.